ISSN 1063-7788, Physics of Atomic Nuclei, 2021, Vol. 84, No. 2, pp. 184–189. © Pleiades Publishing, Ltd., 2021.
Russian Text © The Author(s), 2021, published in Yadernaya Fizika, 2021, Vol. 84, No. 2, pp. 143–148.

ELEMENTARY PARTICLES AND FIELDS
Experiment

Searches for New Physics in the Dilepton Channel with the CMS Detector at the Large Hadron Collider

I. A. Zhizhin[1),2)*, A. V. Lanyov[1), and S. V. Shmatov[1),2)***]**

Received May 13, 2020; revised September 15, 2020; accepted September 15, 2020

Abstract—Results of searches for signals from new physics beyond the Standard Model in proton–proton collisions at the c.m. energy of $\sqrt{s} = 13$ TeV are surveyed. Dilepton-production events detected by the CMS experiment during Run 2 of the Large Hadron Collider (LHC) are used in these searches. The total amount of the data under analysis corresponds to an integrated luminosity of up to 140 fb^{-1}. The results in question were interpreted within models of an extended gauge sector, scenarios of low-energy gravity, and in the context of searches for dark-matter particles. The results of searches for the rare Higgs boson decay to two muons are also discussed.

DOI: 10.1134/S1063778821010245

Investigation of dilepton-production processes is one of the priority lines of research in experiments at modern accelerator complexes—in particular, experiments at the Large Hadron Collider (LHC). Such experimental signals are of particular interest since they stem from very pure channels from the point of view of background conditions described by the Standard Model to a high degree of precision. Apart from being a proving ground in testing Standard Model predictions [1], these processes have been used for several decades as a tool of paramount importance in searches for new-physics signals [2].

Many scenarios beyond the Standard Model predict the appearance of new particles, which thereupon decay to l^+l^- dileptons. Since the energy scale of new physics is expected to be rather high (about 1 TeV and above), final dilepton states are predicted to possess a large invariant mass. A verification of such predictions is within the potential of experiments at the LHC—during Run 2 of its operation, the center-of-mass (c.m.) energy of colliding protons was $\sqrt{s} =$ 13 TeV, while the total amount of the data recorded by either multipurpose experiment (ATLAS and CMS) exceeded 140 fb^{-1} of integrated luminosity. Either experiment is aimed at testing the Standard Model in the region of TeV energies and at searching for new physics beyond it—in particular, in dileptonic channels. Searches for respective signals are performed under the assumption that they are an excess of the observed number of events above the Standard Model background: either within a narrow interval of dilepton invariant masses (new narrow resonance states) or over a broad invariant-mass range (nonresonance signals) [3].

In the Compact Muon Solenoid (CMS) experiment [4], the maximum-likelihood method is applied in searches for new resonances [5, 6] via an analysis of the invariant-mass (m) distribution of dileptons (see Fig. 1) [7]. This approach yields results that are independent of the error in determining absolute background values. The extended maximum-likelihood function for the invariant-mass spectrum is the sum of the probability-density functions for the signal, p_S, and for the background, p_B; that is,

$$L(m|R_\sigma, M, \Gamma, \sigma(m), \alpha, \beta, \kappa, \mu_B) \tag{1}$$
$$= \frac{\mu^N e^{-N}}{N!} \prod_{i=1}^{N} \left(\frac{\mu_S(R_\sigma)}{\mu} p_S(m_i|M, \Gamma, \omega) + \frac{\mu_B}{\mu} p_B(m_i|\alpha, \beta, \kappa) \right).$$

The signal probability-density function $p_S(m|\Gamma, \sigma) = \mathrm{BW}(m|\Gamma) \otimes \mathrm{Gauss}(m|\omega)$ is the convolution of a nonrelativistic Breit–Wigner form describing the resonance under study and having a width Γ and a Gaussian function of width ω that specifies the resolution of the detector systems used. Here, N is the total number of detected events and $\mu = \mu_S + \mu_B$ is the sum of the average values of the Poisson distributions for the signal and background. The form of the background probability-density function was fixed on the basis of approximating distributions of events obtained by

1)Joint Institute for Nuclear Research, Dubna, Russia.
2)Dubna State University, Dubna, Russia.
*E-mail: ilia.zhizhin@cern.ch
**E-mail: alexander.lanyov@cern.ch
***E-mail: sergei.shmatov@cern.ch

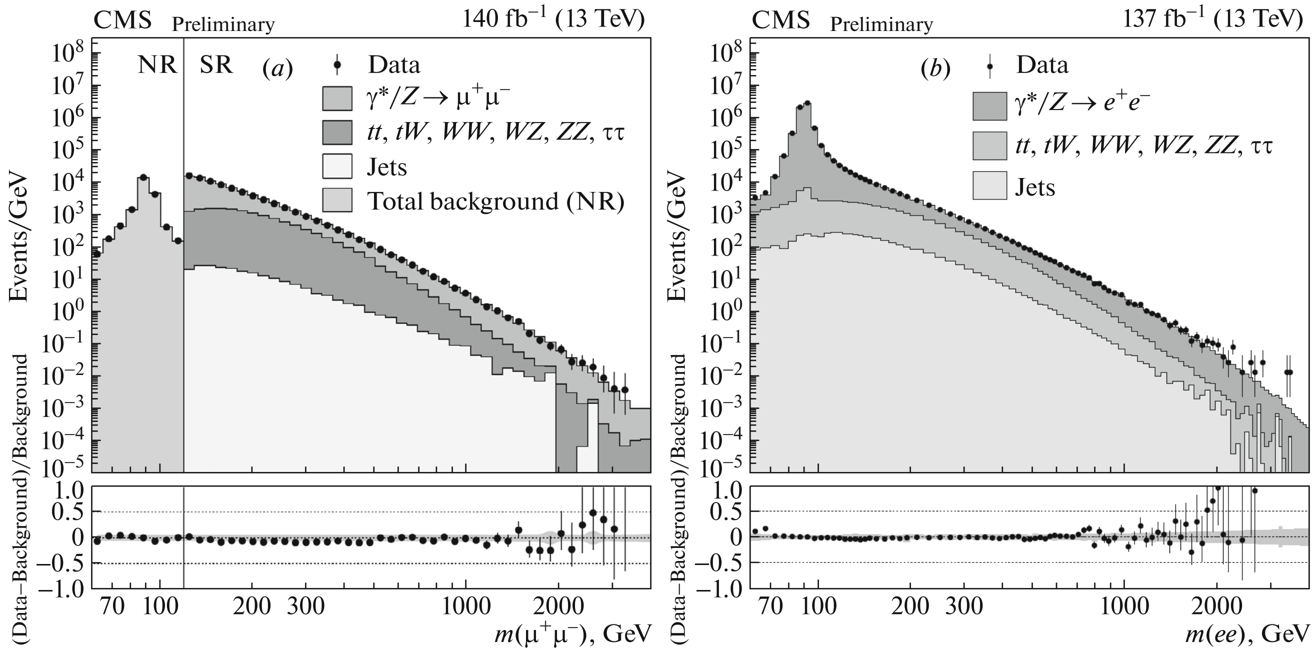

Fig. 1. Invariant-mass distributions of (closed circles) observed (*a*) dimuon and (*b*) dielectron events [7]. The histograms show the contributions of various Standard Model background processes. The gray region of the dimuon distribution is the $m_{ll} < 120$ GeV normalized region (NR).

means of simulating all possible Standard Model processes; that is, $p_B(m|\alpha, \beta, \kappa) = m^{\kappa} e^{\alpha m + \beta m^2}$, where α, β, and κ are the background-shape parameters.

In order to reduce the influence of other systematic effects (luminosity, acceptance, and efficiencies of the trigger and off-line reconstruction), the dilepton-production cross section was normalized to the cross section for Z-boson production (for more details, see, for example, [3]):

$$R_\sigma = \frac{\sigma(Z' \to l^+l^-)}{\sigma(Z \to l^+l^-)}. \qquad (2)$$

The upper limits on the cross sections for the production of spin-1 and spin-2 resonance states according to expectations based on the Standard Model predictions and according to observations are shown in Fig. 2 [7, 8]. These limits, as well as invariant-mass distributions in Fig. 1, show good agreement with the Standard Model predictions—that is, the absence of any statistically significant signals from new physics. Therefore, further results are associated with constraining the parameters of the models within which the predictions were compared with the experimental data. This interpretation of the results is implemented for models of two classes—those that predict spin-1 resonances and those that predict spin-2 resonances.

By way of example, we indicate that, in extended gauge models involving the extra gauge group $U'(1)$, new gauge bosons Z' (spin-1 resonances) of mass measurable at the LHC appear owing to symmetry breaking at a TeV scale [9]. Two models predicting Z' with a maximal and a minimal cross section were used for analysis. As a model with a maximal cross section, one usually considers the so-called Sequential Standard Model (SSM) [10], which is a Standard Model structure derivative where the coupling constant of the new Z' boson is identical to that for the Z boson in the Standard Model. Other models, such as those based on the Grand Unified Theory (GUT) gauge group E_6 [11], predict Z' with coupling constants different from those in the Standard Model and with smaller cross sections. One possible model (Z'_ψ) with a minimal cross section was used as the most pessimistic scenario (lower limit on theoretical predictions). The corresponding cross sections are given in Fig. 2*a* [7]. The lower limits on the Z'_{SSM} and Z'_ψ masses are, respectively, 5.15 and 4.56 TeV/c^2 (that is, the experimental data exclude the existence of Z' of mass less than these values).

The Narrow Width Approximation (NWA) [12, 13] was used to obtain model-independent results that would make it possible to perform their direct reinterpretation within a large number of models. In this approach, the on-shell new-resonance cross section was calculated within the mass interval corresponding to $\pm 5\%\sqrt{s}$ around the respective resonance mass M, while the Z-boson cross section was calculated within the interval ± 30 GeV/c^2 around the Z-boson

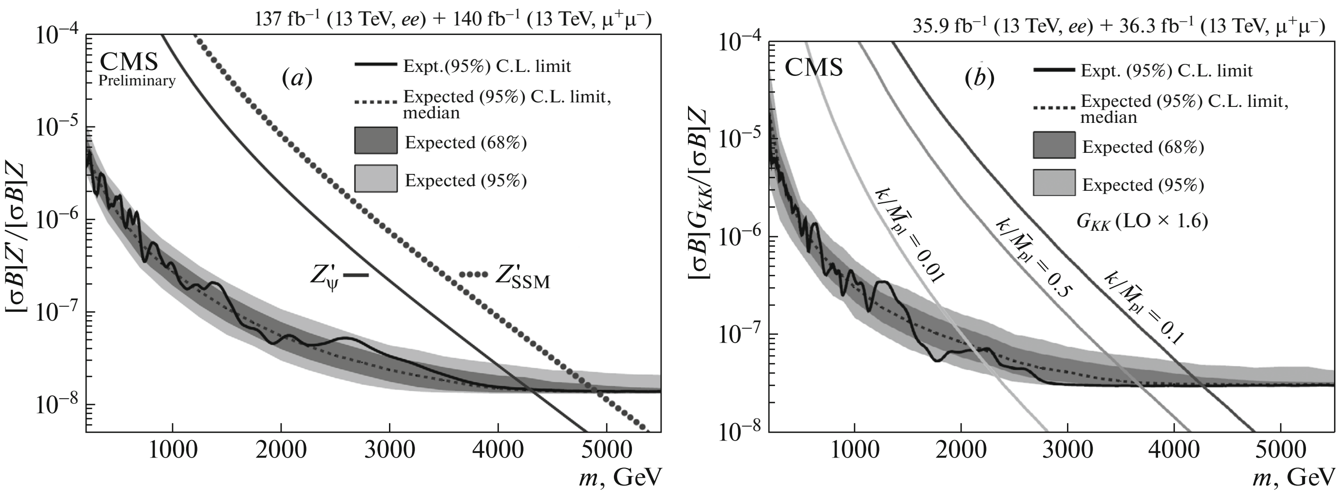

Fig. 2. Upper limits on the dilepton-production cross sections at a confidence level (C.L.) of 95% after a normalization to the Z-boson-production cross section for (a) spin-1 [7] and (b) spin-2 [8] resonances. The solid curves represent the observed limits, while the dotted curves correspond to those that are expected within the Standard Model. The shaded regions around the dashed curve correspond to 68% and 95% quantiles for the expected limit. Also shown in this figure are the cross sections for the production of (a) new gauge bosons in the Z'_ψ and $Z'_{\rm SSM}$ models and (b) RS1 gravitons having the coupling-constant values of $k/\overline{M}_{\rm Pl} = 0.01$, 0.05 and 0.10.

mass. This choice permits minimizing the influence of model-dependent effects, such as the interference-induced modification of the mass-distribution tail in the region below $\sqrt{\hat{s}}$—for example, $\gamma/Z/Z'$ (the interference changes the cross-section value by not more than a few percent). It is noteworthy here that, according to [14], fulfillment of the NWA condition requires the smallness of the natural resonance width Γ in relation to the resonance mass ($\Gamma \ll M$) and the smallness of the mass itself in relation to the interaction energy ($M \ll \sqrt{s}$). Also, there should be no significant interference with nonresonance signals.

In the NWA framework, the cross section for Z'-boson production can be expressed in terms of the vector-boson couplings to quarks as [8, 13]

$$\sigma_{l^+l^-} = \frac{\pi}{48s}\left[c_u w_u(s, M^2) + c_d w_d(s, M^2)\right],$$

where c_u and c_d are coefficients that depend on the Z'-boson couplings to, respectively, up and down quarks. The coefficients w_u and w_d carry information about the parton distributions and are model-independent quantities, since they depend only on the interaction energy $\sqrt{s}$ and on the boson mass $M_{Z'}$. Thus, we see that, in the NWA framework and under the condition that the natural resonance width does go beyond the mass resolution of the detector systems used, the above approach makes it possible to extrapolate resulting constraints to other models in the (c_u, c_d) space as well (see Fig. 3) [8].

The predictions of the Randall–Sundrum scenario (RS1) [15] featuring extra spatial dimensions are traditionally considered as an example of spin-2 resonances. This popular model of low-energy gravity was proposed in order to solve the problem of a large difference between the energy scale of electroweak-symmetry breaking, $M_{\rm EW}$, and the gravity energy scale $M_{\rm Pl}$ (hierarchy problem). Via introducing extra spatial dimensions, it turns out to be possible to reduce the upper energy scale from the Planck value to a substantially lower value, with the result that it approaches $M_{\rm EW}$, whereupon the hierarchy of scales disappears as such. Within this approach, there arise four-dimensional Kaluza–Klein (KK) excitations of those particles that may propagate in extra dimensions (in the simplest versions of such models, these are gravitons alone). The excited states of RS1 gravitons look like spin-2 resonance states in the particle-spectrum of the Standard Model (in particular, leptons).

Figure 2b gives the expected and observed limits on the production cross sections for the first KK mode of RS1 gravitons with various coupling constants $c = k/\overline{M}_{\rm Pl}$ (and, accordingly, with various widths), where k is the radius of curvature of five-dimensional anti-de Sitter space and $\overline{M}_{\rm Pl}$ is the fundamental Planck mass [8]. The limits on the RS1-graviton mass turned out to be 2.10, 3.65, and 4.25 TeV/c^2 for, respectively, $c = 0.01$, 0.05, and 0.10 [16].

During RUN2, the results of searches for new heavy dilepton resonances were interpreted for the first time in the context of signals from particles treated as candidates for dark-matter (DM) particles.

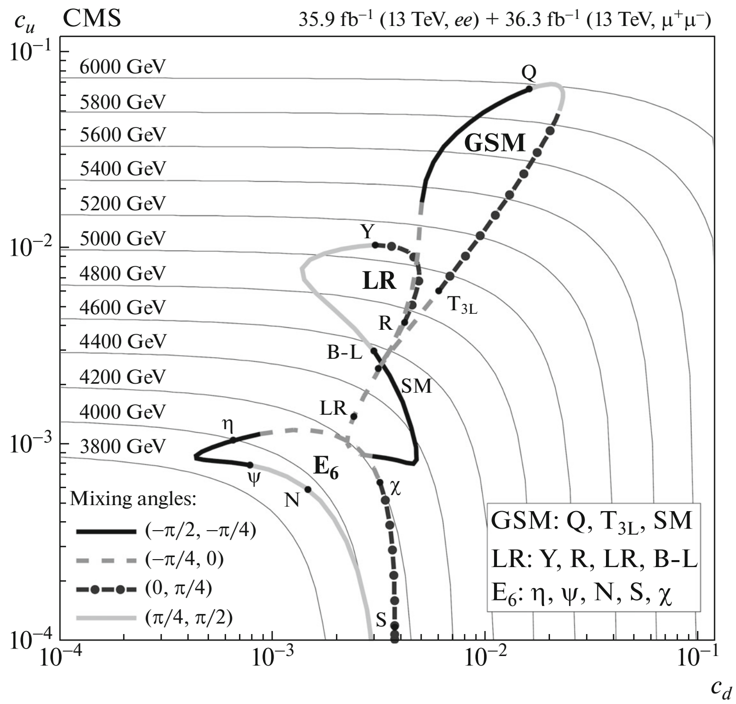

Fig. 3. Limit (at a 95% C.L.) on the Z'-boson masses in the (c_u, c_d) parameter space [8]. Thin lines show contours of the experimental upper limits on (c_u, c_d) for various resonance masses. Thick curves correspond to predictions of various extended gauge models.

For this, use was made of a simplified model featuring one DM particle and one carrier of interaction between the SM and DM sectors [17], where the carrier may be a vector or an vector particle. Two cases where considered—one where the couplings of the axial-vector interaction carriers to leptons and quarks are identical ($g_q = g_l = 0.1$) and the other where the coupling of the axial-vector interaction carrier to leptons is suppressed ($g_q = 0.1$ and $g_l = 0.01$) and which is referred to as the case of "leptophobic" decay. Figure 4 shows the resulting limits on the masses of DM particles [8].

As for nonresonance signals, the procedure for their searches relies on counting the number of events in a specific mass interval. The probability for observing $N_{\rm Obs}$ events is determined by the Poisson distribution

$$\mathcal{P} = \frac{a^{N_{\rm Obs}}}{N_{\rm Obs}!}e^{-a}, \tag{3}$$

where a is the average value of the distribution. This value includes the contributions of the cross sections for signal, σ_S and background, σ_B, processes; the total efficiencies of reconstruction, ε_S, and selection, ε_B; and the normalization of the invariant-mass spectrum to the number of events around the Z-boson peak. Ultimately, we have $a = (\varepsilon_S\sigma_S + \varepsilon_B\sigma_B)N_{{\rm Obs},Z}/(\varepsilon_Z\sigma_Z)$ [18].

Experimental data were interpreted in the context of interactions that predict a nonresonance modification of the shape of dilepton distributions with respect to the Standard Model predictions over a wide region of invariant masses. For example, upper limits on the cross sections for processes involving a virtual exchange of ADD gravitons were set within the low-energy gravity scenario involving flat extra spatial dimensions [19] where use is made of an effective four-fermion description of interaction. Within various renormalization schemes [20–22], new experimental limits on the fundamental scale Λ_T and on M_S were obtained for various numbers of extra spatial dimensions (see Fig. 5*a*) [16]. Moreover, a nonresonance enhancement of massive-dilepton production is also possible within the scenario of Contact Interactions (CI) [23] that arise under the assumption that fermions have a nontrivial structure. The results of CI searches are represented in the form of limits on the energy scale Λ_T (Fig. 5*b*) [16] below which the fermion constituents are bound into singlet states with respect to the new interaction.

In conclusion, we will dwell upon yet another possible window to new physics—rare Higgs boson decay to a dimuon. For this decay, the Standard Model predicts the branching ratio of $\mathcal{B}_{\rm SM}(H \to \mu^+\mu^-) = 2.18 \times 10^{-4}$. All properties of the Higgs boson have so far appeared to be in good agreement with the

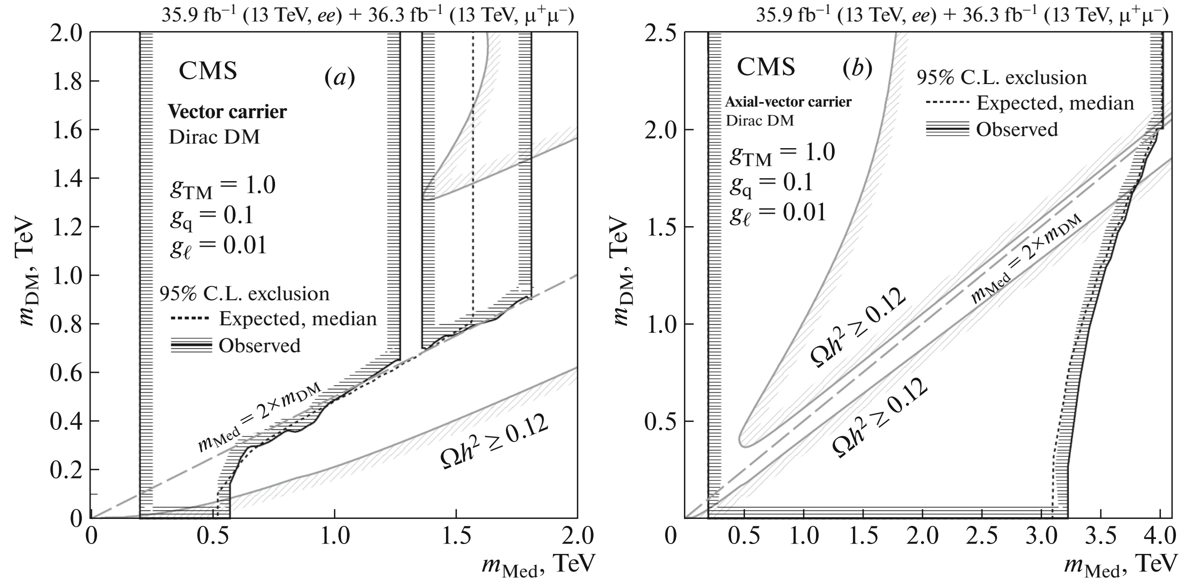

Fig. 4. Limits (at a 95% C.L.) on the mass of dark-matter (DM) particles in (a) the model featuring one vector interaction carrier and (b) the model featuring one axial-vector interaction carrier [8]. The region singled out by a horizontal hatching is excluded for the carrier masses and the masses of DM particles. The gray solid lines with inclined hatching, which carry the "$\Omega h^2 \geq 0.12$" label, correspond to the parameter values that reproduce the observed relic density of dark matter in the Universe. The hatching zone specifies regions where the DM density reconstructed on the basis of the simplified DM model exceeds the observed relic DM density in the Universe.

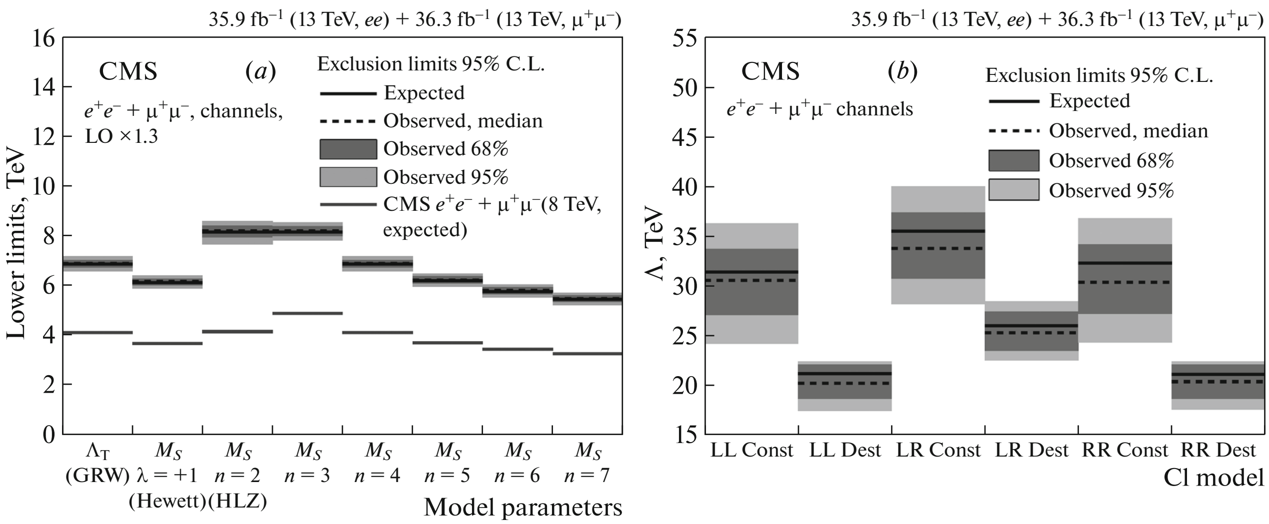

Fig. 5. (a) Limits (at a 95% C.L.) on the fundamental scale of gravity in the ADD scenario within various renormalization schemes [16]; (b) limits (at a 95% C.L.) on the fundamental scale Λ for six Contact Interaction (CI) models considered in [16].

Standard Model predictions. However, rare decays that are not forbidden within the Standard Model and which have not yet been observed prevent an unambiguous conclusion as to whether the Higgs boson is fully a Standard Model particle (in addition, it is worth mentioning here that, for "invisible" decays forbidden in the Standard Model, there is still a window of possibilities at a branching-ratio level of $\mathcal{B}(H \to \text{inv}) \lesssim 20\%$).

In 2020, the CMS Collaboration published a new article [24] devoted to Higgs boson decay to a dimuon. These results were obtained by combining four independent channels of Higgs boson production: gluon–gluon fusion, WW and ZZ vector-boson fusion (VBF), HW and HZ associated production with vector bosons (HV), and associated production with a top-quark pair (ttH). An excess of events in data is observed at a level of 3.0 standard deviations (3.0σ).

At the same time, the statistical significance expected within the Standard Model for the Higgs boson of mass m_H =125.35 GeV is 2.5σ. The measured signal strength with respect to the expectation in the Standard Model is $1.19^{+0.40}_{-0.39}(\text{stat.})^{+0.15}_{-0.14}(\text{syst.})$. These results are of key importance for fundamental physics, since they pave the way toward studying Higgs boson coupling to second-generation fermions.

REFERENCES

1. S. V. Shmatov, Phys. Part. Nucl. **48**, 796 (2017); Phys. At. Nucl. **78**, 509 (2015); I. N. Gorbunov and S. V. Shmatov, Phys. At. Nucl. **78**, 603 (2015); A. V. Lanyov, Phys. Usp. **57**, 923 (2014); I. N. Gorbunov and S. V. Shmatov, Phys. At. Nucl. **76**, 1100 (2013).
2. S. V. Shmatov, Phys. Part. Nucl. **49**, 735 (2018); A. V. Lanyov, Phys. Part. Nucl. **48**, 779 (2017); S. V. Shmatov, Phys. At. Nucl. **79**, 266 (2016); **76**, 1106 (2013); **74**, 490 (2011); A. V. Lanyov, Phys. At. Nucl. **78**, 521 (2015); I. A. Golutvin and S. V. Shmatov, Phys. Part. Nucl. **48**, 720 (2017);
3. A. B. Zarubin, A. V. Lanev, M. V. Savina, and S. V. Shmatov, in *Essays on Modern Particle Physics* (OIYaI, Dubna, 2020), p. 290 [in Russian]; M. V. Savina and S. V. Shmatov, in *Physics of XXI Century As Seen by the Eyes of Creators of the Experimental Complex at LHC in Geneva* (Eterna, Moscow, 2009), p. 437 [in Russian].
4. CMS Collab. (G. L. Bayatian et al.), CERN/LHCC 2006-001 (2006).
5. CMS Collab. (V. Khachatryan et al.), J. High Energy Phys. **1504**, 025 (2015).
6. Particle Data Group (M. Tanabashi et al.), Phys. Rev. **98**, 030001 (2018).
7. CMS Collab., CMS-PAS-EXO-19-019.
8. CMS Collab. (A. M. Sirunyan et al.), J. High Energy Phys. **1806**, 120 (2018).
9. A. Leike, Phys. Rep. **317**, 143 (1999).
10. G. Altarelli, B. Mele, and M. Ruiz-Altaba, Z. Phys. C **45**, 109 (1989); Z. Phys. C **47**, 676(E) (1990).
11. J. L. Hewett, and T. G. Rizzo, Phys. Rep. **183**, 193 (1989).
12. M. Carena et al., Phys. Rev. **70**, 093009 (2004).
13. E. Accomando et al., Phys. Rev. **83**, 075012 (2011).
14. D. Berdine, N. Kauer, and D. Rainwater, Phys. Rev. Lett. **99**, 111601 (2007); N. Kauer, Phys. Lett. B **649**, 413 (2007); C. Uhlemann and N. Kauer, Nucl. Phys. B **814**, 195 (2009).
15. L. Randall and R. Sundrum, Phys. Rev. Lett. **83**, 4690 (1999).
16. CMS Collab. (A. M. Sirunyan et al.), J. High Energy Phys. **04**, 114 (2019).
17. A. Albert, M. Backovic, A. Boveia, O. Buchmueller, G. Busoni, A. de Roeck, C. Doglioni, T. Du Pree, M. Fairbaim, M.-H. Genest, S. Gori, G. Gustavino, K. Hahn, U. Haisch, P. C. Harris, and D. Hayden, Phys. Dark Univ. **26**, 100377 (2019).
18. CMS Collab. (V. Khachatryan et al.), J. High Energy Phys. **1504**, 025 (2015).
19. N. Arkani-Hamed, S. Dimopoulos, and G. R. Dvali, Phys. Lett. B **429**, 263 (1998).
20. G. F. Giudice, R. Rattazzi, and J. D. Wells, Nucl. Phys. B **544**, 3 (1999).
21. J. L. Hewett, Phys. Rev. Lett. **82**, 4765 (1999).
22. T. Han, J. D. Lykken, and R.-J. Zhang, Phys. Rev. D **59**, 105006 (1999).
23. E. Eichten, K. D. Lane, and M. E. Peskin, Phys. Rev. Lett. **50**, 811 (1983).
24. CMS Collab. (A. M. Sirunyan et al.), arXiv:2009.04363; CMS Collab. (2020, in press).